EFFECT OF AN INSERTED POROUS LAYER ON HEAT AND FLUID FLOW IN A VERTICAL CHANNEL WITH MIXED CONVECTION

by

Hasan CELIK and Moghtada MOBEDI *

Department of Mechanical Engineering, Izmir Institute of Technology, Urla, Izmir, Turkey

Original scientific paper
DOI: 10.2298/TSCI121001056C

Temperature and velocity fields in a vertical channel partially filled with porous medium under mixed convection heat transfer condition are obtained. The heat transfer equation and equation of motion for clear and porous layer regions are written and solved analytically. The non-dimensionalization of the governing equations yields two Grashof numbers as Gr_c and Gr_d for clear and porous sections where $Gr_d = Da \cdot Gr_c$. The dimensionless governing parameters for the problem are Gr_c (or Gr_d), Da, thermal conductivity ratio, and thickness of porous layer. The temperature and velocity profiles for different values of Gr_c, Da, thermal conductivity ratio, and thickness of porous layer are plotted and their changes with the governing parameters are discussed. Moreover, the variation of pressure drop with the governing parameters is investigated. The decrease of porous layer thickness or thermal conductivity ratio increases the possibility of the downward flows. Thermal conductivity ratio plays important role on pressure drop, particularly for the channels with high values of Gr_c/Re.

Key words: *mixed convection, porous medium, partially porous filled channel*

Introduction

Mixed convection in heated channels has received attention of researchers due to its application in many practical areas such as nuclear reactors, cooling of electronic equipment, and heat exchangers. The momentum and heat transfer equations for fully developed mixed convection are different than the equations of fully developed forced convection since the fluid velocity is function of temperature. For a fixed fluid flow rate to a vertical channel, the buoyancy results in the flow reversals since fluid in the region near the hot wall receives an extra force (buoyancy force) and a reversal flow occurs in the region near the cold wall. The occurrence of flow reversals was observed by Sparrow, *et al*. [1]. The flow analysis of mixed convection was discussed in the work of Ostrach [2], and Lietzke [3]. Aung and Worku [4] presented the results for fully developed mixed convection flow between in a parallel plate channel in which the net through-flow rate is constant. They found that when the wall temperatures are unequal, a reversed flow situation occurs if the magnitude of the buoyancy parameter Gr/Re exceeds a certain value. Aung and Worku [5] also studied the mixed convection in ducts with asymmetric wall heat fluxes. Their study was performed on the fully developed pure fluid channel and aiding buoyancy forces. They found that the flow reversal is more prone to occur in uniform wall heat fluxes. An analysis of mixed convective flow in a partially filled porous channel was stud-

* Corresponding author; e-mail: moghtadamobedi@iyte.edu.tr

ied by Kumar *et al.* [6]. Three types of thermal boundary conditions as isothermal-isothermal, isoflux-isothermal, and isothermal-isoflux for the left and right walls of the channel were considered. The problem of aiding and opposing mixed convection in a vertical porous layer with a finite wall heat source was investigated by Lai *et al.* [7]. They studied numerically two-dimensional, steady mixed convection in a vertical porous layer for a case when a finite isothermal heat source is located on one vertical wall and the other vertical wall is isothermally cooled. The combined free and forced convection of a fully developed Newtonian fluid within a vertical channel composed of porous medium with viscous dissipation effects was studied by Al-Hadhrami *et al.* [8]. The fourth-order ordinary differential equation, which contains the Darcy and the viscous dissipation terms, was solved analytically by using perturbation techniques and numerical method. Umavathi *et al*. [9] studied the problem of mixed convection in a vertical channel filled with porous media including inertial forces. They considered isothermal-isothermal, isoflux-isothermal boundary conditions. Fully developed mixed convection with viscous dissipation in a vertical channel filled with a porous medium was analyzed analytically for buoyancy aided and opposing flow and for isothermal and isoflux boundary conditions by Barletta *et al*. [10]. The mechanical and thermal characteristics of the flow configurations were investigated both analytically and numerically in this study. Furthermore, buoyancy aided and opposing flows were analyzed numerically for a vertical porous channel with isothermal and isoflux boundary conditions in the case of a fully developed flow by Barletta *et al*. [11]. They concluded that for upward driven flows, the combined effects of viscous dissipation and pressure work may produce a net cooling of the fluid even in the case of a positive heat input from the isoflux wall. Chang and Chang [12] numerically analyzed the developing mixed convection in a vertical tube partially filled with porous medium. Inertia and boundary effects were included in their studies. Furthermore, Mokni *et al.* [13] studied turbulent mixed convection in a heated vertical channel whose walls are subject to a constant heat flux. Mokni *et al.* [14] also studied turbulent mixed convection in an asymmetrically heated vertical channel. Chatterjee and Raja [15] investigated mixed convection heat transfer around five in-line isothermal square cylinders that periodically arranged within a vertical duct. The walls of vertical duct are assumed to be insulated. Celik and Mobedi [16] analyzed mixed convection in three vertical channels as fully filled clear fluid, fully filled fluid saturated porous medium, and half porous layer filled channel. They found analytical expressions for velocity, temperature, and heat function.

The aim of the present study is to obtain the velocity and temperature profiles in a mixed convection vertical channel partially filled with porous media for different porous layer thickness, Darcy number and thermal conductivity ratio. The dimensional forms of the governing equations are solved numerically. Moreover, the governing equations are made dimensionless and analytical solutions are obtained. The results of two approaches are compared to each other to be sure of the obtained analytical expressions. The condition of channel is similar to the channel of previous study of authors [16]; however the porous layer thickness is changed. The present study focused on both heat transfer and pressure drop through the channel by inserting of a porous layer. Based on the obtained results, the change of velocity and temperature distributions for the channels with different values of Gr_c/Re, K, and Da numbers are plotted and discussed. Moreover, the changes of the dimensionless pressure drop and heat transfer rate with the governing parameters are investigated.

The considered channel

Mixed convection in the vertical channel shown in fig. 1 is studied. The channel is partially filled with porous media. The thickness of porous layer is taken as δ. The fluid flowing

through the channel is Newtonian and incompressible. The fluid flow is laminar, fully developed, and steady. The channel walls are maintained at constant temperature of T_c and T_h. The channel has a rectangular cross-section with width of b. It is assumed that the plates are infinitely long in depth direction; the fluid flows in x-direction while y is perpendicular to the flow direction. The fluid properties are constant except the density in buoyancy term of the momentum equation. Viscous dissipation and radiation heat transfer are neglected and gravity acts in x-direction. The porous medium is saturated with fluid and thermal equilibrium between solid and fluid exits.

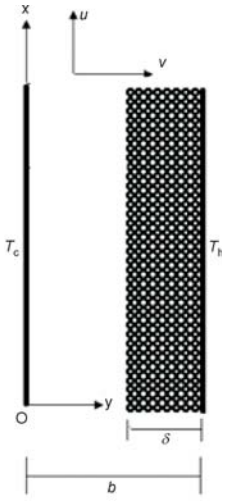

Figure 1. The considered channel

Governing equations and solutions

Velocity, temperature and pressure field

The continuity, momentum, and energy equations for clear fluid section of a fully developed mixed convection heat transfer in a vertical channel, shown in fig. 1, under the Boussinesq's approximation can be written as:

$$\frac{\partial u}{\partial x}=0 \tag{1}$$

$$\mu_{\mathrm{f}}\frac{\mathrm{d}^2u}{\mathrm{d}y^2}-\frac{\mathrm{d}p}{\mathrm{d}x}+\rho g\beta(T-T_{\mathrm{av}})=0 \tag{2}$$

$$\frac{\mathrm{d}^2T}{\mathrm{d}y^2}=0 \tag{3}$$

and for porous section:

$$\frac{\partial u}{\partial x}=0 \tag{4}$$

$$\mu_{\mathrm{eff}}\frac{\mathrm{d}^2u}{\mathrm{d}y^2}-\frac{\mu_{\mathrm{f}}}{K}u+\rho g\beta(T-T_{\mathrm{av}})-\frac{\mathrm{d}p}{\mathrm{d}x}=0 \tag{5}$$

$$\frac{\mathrm{d}^2T}{\mathrm{d}y^2}=0 \tag{6}$$

The dimensional boundary conditions for the governing equations of clear fluid defined in eqs. (1) to (3) can be expressed as:

– on the left side $y=0$ $u(0)=0,\quad T(0)=T_c$ (7)

– at interface $y=b-\delta;$ $u(b)=0=u_{\mathrm{i}};\quad T(b-\delta)=T_{\mathrm{i}}$ (8)

and the dimensional boundary conditions for porous medium layer section can be given as:

– at interface $y=b-\delta;$ $u(b-\delta)=u_{\mathrm{i}};\quad T(b-\delta)=T_{\mathrm{i}}$ (9)

– on the right side; $y=0$ $u(b)=0,\quad T(b)=T_{\mathrm{h}}$ (10)

where T_{i} and u_{i} are temperature and velocity at the porous and clear fluid interface. Brinkman-Darcy equation is used to describe motion of fluid in the porous layer of the channel. A detailed discussion on the choice of the reference fluid temperature for fully-developed mixed

convection in a vertical channel was done by Barletta and Zanchini [17]. They proposed that the mean fluid temperature in a cross-section as the reference fluid temperature for fully developed mixed-convection problems in the channels. Hence, the momentum and energy equations can be non-dimensionalized as:

$$\frac{\mathrm{d}^2U}{\mathrm{d}Y^2}+\frac{\mathrm{Gr}_c}{\mathrm{Re}}\theta-\Gamma=0 \tag{11}$$

$$\frac{\mathrm{d}^2\theta}{\mathrm{d}Y^2}=0 \tag{12}$$

and for porous section:

$$\frac{\mathrm{d}^2U}{\mathrm{d}Y^2}-\frac{M}{\mathrm{Da}}U+M\frac{\mathrm{Gr}_\mathrm{d}}{\mathrm{Re}}\theta-M\Gamma=0 \tag{13}$$

$$\frac{\mathrm{d}^2\theta}{\mathrm{d}Y^2}=0 \tag{14}$$

where $\mathrm{Gr_d} = g\beta K(T_\mathrm{h} - T_\mathrm{c})b/\nu^2$ which is the Darcy modified Grashof number. The Reynolds, Grashof numbers, and Γ are defined as:

$$\mathrm{Re}=\frac{u_0 b}{\nu};\quad \mathrm{Gr_c}=\frac{g\beta(T_\mathrm{h}-T_\mathrm{c})b^3}{\nu^3},\quad \Gamma=\frac{\mathrm{d}P}{\mathrm{d}X} \tag{15}$$

where u_0 is inlet velocity to the channel. In the relations, following parameters are used to make the momentum and energy equations non-dimensionalized:

$$X=\frac{x}{b},\ Y=\frac{y}{b},\ U=\frac{u}{u_0},\ \theta=\frac{T-T_\mathrm{av}}{T_\mathrm{h}-T_\mathrm{c}},\ P=\frac{pb}{u_0\mu_\mathrm{f}},\ \xi=\frac{\delta}{b} \tag{16}$$

The dimensionless boundary conditions for the left half of the channel can be expressed as:

– on the left side $Y = 0$; $U(0)=0,\quad \theta(0)=-0.5$ (17)

– at interface $Y = 1-\xi$ $U(1-\xi)=U_\mathrm{i},\quad \theta(1-\xi)=\theta_\mathrm{i}$ (18)

and the dimensionless boundary conditions for porous medium layer section can be given as:

– at interface $Y = 1-\xi$ $U(1-\xi)=U_\mathrm{i},\quad \theta(1-\xi)=\theta_\mathrm{i}$ (19)

– on the right side $Y = 1$ $U(1)=0,\quad \theta(1)=0.5$ (20)

where U_i and θ_i are the dimensionless velocity and temperature at the interface and ξ is the dimensionless porous layer thickness. The solution of dimensionless heat transfer equation with boundary conditions given in eq. (17) and (18) for clear fluid layer can be written as:

$$\theta_\mathrm{c}(Y)=\frac{\left(\theta_\mathrm{i}+\frac{1}{2}\right)Y}{1-\xi}-\frac{1}{2} \tag{21}$$

The solution of dimensionless momentum equation, eq. (11) of clear fluid layer with boundary conditions explained in eqs. (17) and (18) is:

$$U_\mathrm{c}=C_1Y+\frac{U_i+Y}{1-\xi}+C_2Y^2-C_3Y^3+\Gamma\left[-\frac{(1-\xi)Y}{2}+\frac{Y^2}{2}\right] \tag{22}$$

where C_1, C_2, and C_3 are constants given in Appendix. The solution of dimensionless heat transfer equation with boundary conditions given in eqs. (19) and (20) for porous layer can be written as:

$$\theta_{\mathrm{p}}(Y)=\frac{\left(\frac{1}{2}-\theta_{\mathrm{i}}\right)Y+\theta_{\mathrm{i}}-\frac{1-\xi}{2}}{\xi} \tag{23}$$

The velocity profile for the porous layer region can be found as:

$$U_{\mathrm{p}}=\frac{1}{2[(1-\xi)-1]s^2}\cosh(s-(1-\xi)s)\left\{\begin{array}{l} M\left[\left(\frac{\mathrm{Gr_d}}{\mathrm{Re}}((1-\xi)+2\theta_{\mathrm{i}}(Y-1)-Y\right)\right]\sinh(s-(1-\xi)s) \\ -2(1-\xi)-1)\Gamma \\ -\xi[C_4\sinh(s(\xi-Y))+C_5\sinh(s-sY)] \end{array}\right\} \tag{24}$$

where C_4, and C_5 are constants given in Appendix. U_{i} and Γ are needed to be found. An equation for Ui can be found by using the continuity of shear stress at the interface.

$$U_i=\frac{\{(1-\xi)M[[-6\xi s^4C_6+4MC_7+C_8\cosh(s-(1-\xi)s)]+sC_9\sinh(s-(1-\xi)s)]\}}{C_{10}\{C_{11}\cosh(s-(1-\xi)s)+4M[6M-3(1-\xi)^2s^2+sC_{12}\sinh(s-(1-\xi)s)]\}} \tag{25}$$

By using the compatibility relation, Γ can be determined as:

$$\Gamma=\frac{\left\{((1-\xi)-1)(1-\xi)s\cosh(s-(1-\xi)s)\left[sC_{13}-24M\frac{\mathrm{Gr_d}}{\mathrm{Re}}\tanh(0.5(s-(1-\xi)s))\right]+MC_{14}\right\}}{-4C_{15}\xi} \tag{26}$$

where C_6 to C_{15} are constants given in Appendix. By using the condition of continuous heat flux at the interface, θ_{i} which is dimensionless, interface temperature can be found as:

$$\theta_{\mathrm{i}}=\frac{K[1-(1-\xi)]-(1-\xi)}{2[K(1-\xi)-K-(1-\xi)]} \tag{27}$$

where K is the thermal conductivity ratio (*i. e.*, $K=k_{\mathrm{f}}/k_{\mathrm{eff}}$).

Heat transfer analysis

For the channel without a porous layer, the heat flux received by the left wall depends on the fluid thermal conductivity and channel width. It can be calculated from the following relation:

$$j_{\mathrm{c}}=\frac{T_{\mathrm{h}}-T_{\mathrm{c}}}{\frac{b}{k_{\mathrm{f}}}} \tag{28}$$

For a channel with a porous layer, the heat flux received by left wall can be found from the relation:

$$j_{\mathrm{cp}}=\frac{(T_{\mathrm{h}}-T_{\mathrm{c}})}{\frac{\delta}{k_{\mathrm{eff}}}+\frac{b-\delta}{k_{\mathrm{f}}}} \tag{29}$$

where k_{eff} and k_{f} are effective thermal conductivity of the porous layer and fluid thermal conductivity. The ratio between two heat fluxes is shown by ε:

$$\varepsilon = \frac{j_{cp}}{j_c} = \frac{1}{(1-\xi)+K\xi} \tag{30}$$

For the values of $\varepsilon > 1$, a heat transfer enhancement exits compared to the channel with clear fluids, while for $\varepsilon < 1$, the decrease of heat transfer rate should be expected. That is why ε is called as heat transfer increment/decrement ratio, in this study [18, 19].

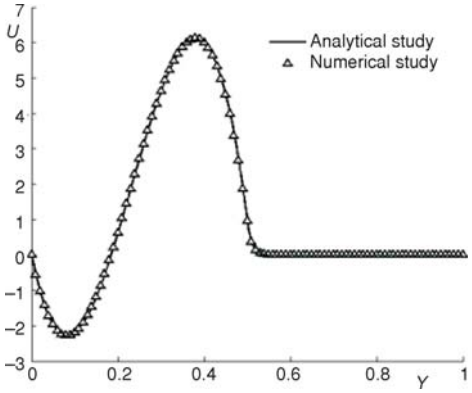

Figure 2. Comparison of numerical and analytical study for ξ = 0.5, Da = 10^{-4}, Gr_c/Re = 2000, and K=100

Results and discussions

The dimensional forms of the governing equations, eqs. (1)-(6), are solved numerically and compared with the analytical solution of the dimensionless forms of the same governing equations Finite difference method is used to solve the motion and energy equations for clear and porous layer regions. Nodal equations are derived for all differential equations and applied to the related nodes in the computational domain. A guess value is assigned to pressure value at all nodes, then the governing equations are solved and mass flow rate is obtained, numerically. If the obtained mass flow is not identical with the initial assigned value, the pressure is changed until the identical values are obtained. A good agreement is observed if 201 × 201 nodes are used. The results of two different approaches (numerical solution for dimensional form and analytical solution for dimensionless form of the governing equations) are compared. Figure 2 shows a sample of comparison results for a channel with ξ = 0.5, Da = 10^{-4}, Gr_c/Re = 2000, and K = 100. As seen, a good agreement between two results is observed.

Temperature and velocity profiles

Figure 3 shows the velocity and temperature profiles for a channel with Gr_c/Re = 1 and 2000, K = 0.05 and three different dimensionless porous thickness of 0.15, 0.5, and 0.85. The temperature profiles are shown in the first row, while the velocity profiles for Gr_c/Re = 1 and 2000 are shown in the second and third rows. For the channel with K = 0.05, the effective thermal conductivity of porous medium is greater than for clear fluid. As a consequence almost a uniform temperature distribution is observed in the porous layer section while a steep temperature gradient is observed in the clear region for the values of ξ = 0.15, 0.50, and 0.85. For the channel with Gr_c/Re = 1, the forced convection is dominant. Therefore, a parabolic velocity profile is observed in the left region of the channel in which no porous medium exists. The magnitude of velocity in the left region increases with the increase of porous layer thickness. The magnitude of velocity in the porous layer (right region) is very smaller than clear fluid region (left region) and almost a uniform velocity exists due to obstacles in the porous medium. The velocity profiles for the channel with Gr_c/Re = 2000 is shown in the third row of fig. 3. The increase of Gr_c/Re from 1 to 2000 causes the increase of buoyancy effect. The magnitude of velocity in the porous layer is very smaller than the clear region and almost a uniform velocity profile is observed in the porous region. For the channel with ξ = 0.85, a parabolic velocity profile is observed in right region. The region in which the clear fluid flows is very narrow and that is why no

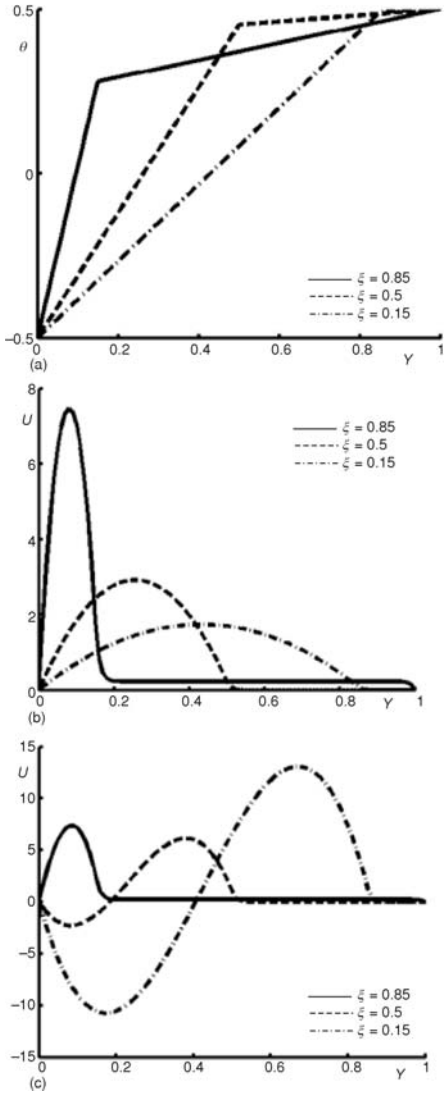

Figure 3. The change of temperature and normalized velocity profiles in the channel with porous layer thickness when Da = 10^{-4} and K = 0.05; (a) temperature distribution, (b) velocity profiles for Gr_c/Re = 1, (c) velocity profiles for Gr_c/Re = 2000

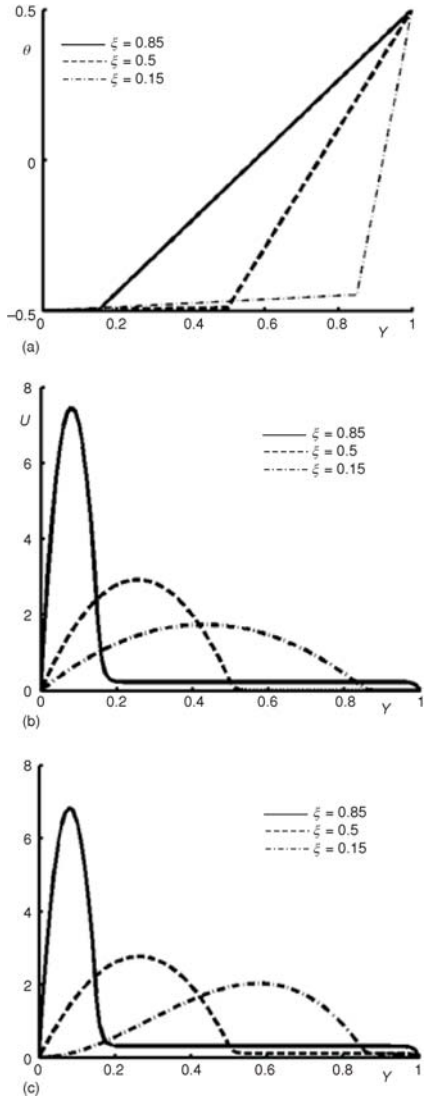

Figure 4. The change of temperature and normalized velocity profiles in the channel with porous layer thickness when Da = 10^{-4} and K = 100; (a) temperature distribution, (b) velocity profiles for Grc/Re = 1, (c) velocity profiles for Gr_c/Re = 2000

downward flow occurs. By reducing of porous layer thickness from 0.85 to 0.50, the thickness of clear fluid region increases and that is why a downward flow is observed in the left region. Further increase of Gr_c/Re causes the increase of buoyancy effect and then strong upward and downward flows occur. The downward flow can be clearly observed for ξ = 0.15.

Figure 4 shows the temperature and velocity profiles in the channel with K = 100, and for three different porous layer thickness as 0.15, 0.50, and 0.85, and two different values of

Gr_c/Re as 1 and 2000. The temperature profiles in the channel with $\xi = 0.15$, 0.50, and 0.85 are shown in the first row of fig. 4. As seen, almost a uniform temperature exits in the right region of the channel due to high value of clear fluid. The value of dimensionless temperature at the interface is –0.5 and it linearly changes from –0.5 to 0.5 in the porous layer. The velocity profiles for $Gr_c/Re = 1$ and for three different values of porous layer thickness are seen in the second row of fig. 4. Due to low value of Gr_c/Re (*i. e*., $Gr_c/Re = 1$), the forced convection is dominant and parabolic velocity profiles are observed in the left region of the channel for three different values of porous layer thickness. By increasing the value of Gr_c/Re from 1 to 2000, no considerable change in the velocity profile is observed since the whole region of the clear fluid is at uniform temperature of –0.5 and no buoyancy effect existence in the clear fluid region.

Our numerical observation shows that even small change of fluid flow rate in the porous layer can considerably influence total pressure drop through the channel. Figure 5(a) shows the velocity profile in the channel with $\xi = 0.5$, K =100 for three values of Gr_c/Re as 1, 1000, and 2000. As it was mentioned before, a uniform temperature exits in clear fluid region and no buoyancy force exits for $K = 100$. By increasing of Gr_c/Re number, the buoyancy forces in porous layer is enhanced and the rate of fluid in the porous increases.

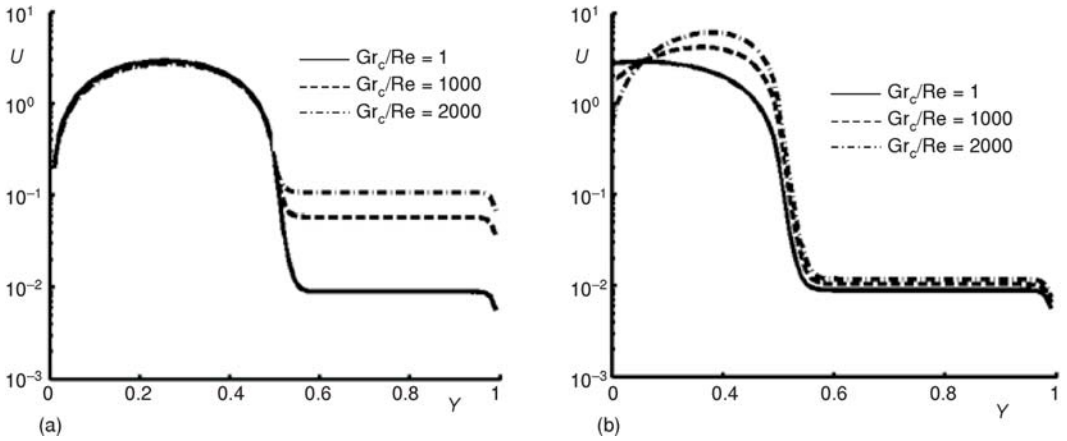

Figure 5. Normalized velocity profile in the channel with $\xi = 0.5$ (a) $K = 100$, (b) $K = 0.05$

As seen from fig. 5(a), the normalized velocity in the porous region is around 0.01 for $Gr_c/Re = 1$ and it increases to 0.1 for $Gr_c/Re = 2000$. Hence, the pressure drop in the channel $Gr_c/Re = 2000$ should be higher than the channel with $Gr_c/Re = 1$. Figure 5(b) shows the normalized velocity profile in the channel with $\xi = 0.5$, $K = 0.05$ for the same values of Gr_c/Re as 1, 1000, and 2000. Due to the negative values of normalized velocity, Y axis is limited between 0.2 and 1. For the channel with $K = 0.05$, a uniform temperature exists in the porous layer while a linear temperature exists in the clear fluid region. As seen, the fluid flow in the porous layer does not increase with increase of Gr_c/Re. However, it causes occurrence of the reverse flow in the clear fluid region. For the channel with $K = 0.05$, no considerable increase of pressure drop in X direction is expected due to two reasons. Firstly, no considerable increase of flow is observed in the porous layer, and secondly the occurrence of reverse flow has negative effect on the increase of pressure drop in positive direction of x.

Results for heat transfer analysis

Figure 6 shows the variation of heat transfer decrement/increment ratio with thermal conductivity ratio for different values of porous layer thickness. As seen, for the channel with clear fluid (*i. e.* $\xi = 0$) the value of ε is 1. By increasing the porous layer thickness, the dimensionless heat transfer flux increases for the region of $K < 1$ while it decreases for large values of thermal conductivity ratio (*i. e.*, $K > 1$). The important point of fig. 6 is that the value of varies only in a region around $K = 1$ and it is almost constant behind or after this region. Hence, after a certain value of thermal conductivity ratio, further increase or decrease of K does not enhance or reduce heat transfer rate.

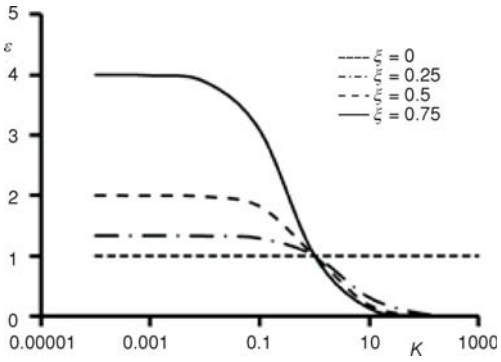

Figure 6. The change of dimensionless heat flow rate with thermal conductivity ratio for different values of porous layer thickness

Results for pressure drop

Figure 7 shows the change of dimensionless pressure drop with Gr_c/Re number for two values of Darcy of 10^{-3}, 10^{-4}, and thermal conductivity ratios of 100 and 0.05. For the thermal conductivity ratio of $K = 100$ and Da $=10^{-3}$, 10^{-4}, the pressure drop increases with increase of Grc/Re since the fluid flow rate increases in the porous layer, fig. 5(a). Moreover, the increase of Da number reduces the dimensionless pressure drop in the channel since fluid can easily flows in the porous layer. For the channel with $K = 0.05$, the increase of pressure drop with Gr_c/Re is negligible and almost a constant pressure drop is observed in the channel for two different values of Gr_c/Re. As it was mentioned before, for the channel with $K = 0.05$, a reverse flow prevents the increase of pressure drop along the channel. Figure 7 shows that the net pressure drop, which is the summation of pressure drop in flow direction (+x) and the pressure drop from top to bottom (–x), is highly influenced from thermal conductivity ratio.

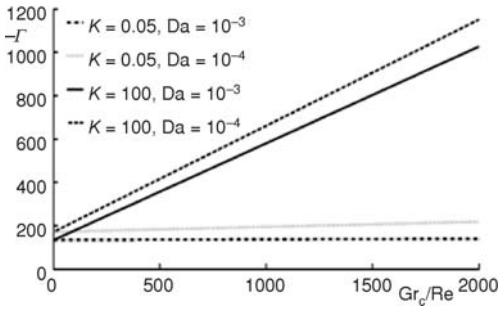

Figure 7. The change of dimensionless pressure drop with Gr_c/Re for channels with different values of K and Da number when $\xi = 0.5$

Conclusions

Fully developed heat and fluid flow in a vertical channel assisted with a porous layer on the right wall for mixed convection heat transfer is analyzed numerically and analytically. The numerical and analytical results are compared and good agreement between results is observed. Based on the obtained results, following remarks can be concluded.

- The velocity profile is highly influenced from thermal conductivity ratio and porous layer thickness. Various velocity profiles can be observed in the channels with the same Grashof number, Darcy number and porous layer thickness but different thermal conductivity ratio.
- The possibility of downward flows increases with decrease of porous layer thickness or increase of effective thermal conductivity of porous layer.

- The increase of thermal conductivity of fluid reduces the buoyancy effect in clear fluid region and consequently the possibility of downward flow is reduced.
- Heat transfer from the hot to cold wall changes only in a region of thermal conductivity ratio around 1. However, after certain values of thermal conductivity ratio, the heat transfer rate is not changed with further increase/decrease of thermal conductivity ratio.
- The pressure drop in the channel is highly influenced from thermal conductivity ratio, particularly at low values of Darcy number (*i. e*., Da = 10^{-4}). Pressure drop in the channel with high thermal conductivity ratio (*i. e*. $K = 100$) is considerably greater than the pressure drop of the channel with the low values of K.

Nomenclature

b – spacing between walls, [m]
C_p – specific heat, [$Jkg^{-1}K^{-1}$]
g – acceleration due to gravity [ms^{-2}]
Gr_c – Grashof number for channel with clear fluid
Gr_d – Grashof number for channel with porous media
j – heat flux, [Wm^{-2}]
k – thermal conductivity, [$Wm^{-1}K^{-1}$]
K – permeability thermal conductivity ratio, [m^2],
M – relative viscosity,($= \mu/\mu_{eff}$)
P – dimensionless pressure
Pe – Peclet number
p – pressure [Pa]
Re – Reynolds number
s – shape parameter
T – temperature, [°C]
u, v – axial and transverse velocity, [ms^{-1}]
U, V – dimensionless axial and transverse velocity
x, y – axial and transverse co-ordinate, [m]
X, Y – dimensionless axial and transverse co-ordinate

Greek symbols

β – coefficient of thermal expansion
Γ – pressure gradient along channel
δ – porous layer thickness, [m]
ε – heat transfer increment/decrement ratio
θ – dimensionless temperature
μ – dynamic viscosity of the fluid, [$kgms^{-1}$]
μ_{eff} – dynamic viscosity for Brinkman's model, [$kgms^{-1}$]
ν – kinematic viscosity of the fluid, [m^2s^{-1}]
ξ – dimensionless porous layer thickness
ρ – density, [kgm^{-3}]

Subscripts

c – cold wall, clear fluid
eff – effective
f – fluid
i – interface
d – Darcy
h – hot wall
av – average
ref – reference value

References

[1] Sparrow, E. M., *et al*., Observed Flow Reversals and Measured-Predicted Nusselt Numbers for Natural Convection in a One-Sided Heated Vertical Channel, *ASME J. Heat Transfer, 106* (1984), 2, pp. 325-332
[2] Ostrach, S., Combined Natural and Forced Convection Laminar Flow Heat Transfer of Fluids with and without Heat Sources in Channels with Linearly Varying Wall Temperatures, *NACA TN, 3141*, 1954
[3] Lietzke, A. F., Theoretical and Experimental Investigation of Heat Transfer by Laminar Natural Convection between Parallel Plates, *NACA, 1223* (1954)
[4] Aung, W., Worku, G., Theory of Fully Developed, Combined Convection Including Flow Reversal, *J. of Heat Transfer, 108* (1986), 2, pp. 485-488
[5] Aung, W., Worku, G., Developing Flow and Flow Reversal in a Vertical Channel with Asymmetric Wall Temperatures, *J. of Heat Transfer, 108* (1986), 2, pp. 299-304
[6] Kumar, J., *et al.*, Fully Developed Mixed Convection Flow in a Vertical Channel Containing Porous and Fluid Layer with Isothermal or Isoflux Boundaries, *Transport in Porous Media, 80* (2009), 1, pp. 117-135
[7] Lai, F. C., *et al.*, Aiding and Opposing Mixed Convection in a Vertical Porous Layer with a Finite Wall Heat Source, *Int. J. of Heat and Mass Transfer, 31* (1988), 6, pp. 1049-1061
[8] Al-Hadhrami, *et al*., Combined Free and Forced Convection in Vertical Channels of Porous Media, *Transport in Porous Media, 49* (2002), 3, pp. 265-289

[9] Umavathi, J., *et al*., Mixed Convection in a Vertical Porous Channel, *Transport in Porous Media, 61* (2005), 3, pp. 315-335
[10] Barletta, A., *et al*., Mixed Convection with Viscous Dissipation in a Vertical Channel Filled with a Porous Medium, *Acta Mechanica, 194* (2007), 1, pp. 123-140
[11] Barletta, A., Nield, D., Combined Forced and Free Convective Flow in a Vertical Porous Channel: The Effects of Viscous Dissipation and Pressure Work, *Transport in Porous Media, 79* (2009), 3, pp. 319-334
[12] Chang, W. J., Chang, W.-L., Mixed Convection in a Vertical Tube Partially Filled with Porous Medium, *Numerical Heat Transfer, Part A: Applications, 28* (1995), 6, pp. 739-754
[13] Mokni, A., *et al*., Turbulent Mixed Convection in Heated Vertical Channel, *Thermal Science, 14* (2010), 1, pp. 125-135
[14] Mokni, A., *et al*., Turbulent Mixed Convection in Asymmetrically Heated Vertical Channel, *Thermal Science, 16* (2012), 2, pp. 503-512
[15] Chatterjee, D., Raja, M., Mixed Convection Heat Transfer Past in-line Square Cylinders in a Vertical Duct, *Thermal Science, 17* (2013), 2, pp. 567-580
[16] Celik, H., Mobedi M., Visualization of Heat Flow in a Vertical Channel with Fully Developed Mixed Convection, *Int. Commun. Heat Mass Transfer, 39* (2012), 8, pp. 1253-1264
[17] Barletta, A., Zanchini, E., On the Choice of the Reference Temperature for Fully-Developed Mixed Convection in a Vertical Channel, *Int. J. Heat Mass Transfer, 42* (1999), 16, pp. 3169-3181
[18] Cekmer, O., *et al*., Fully Developed Forced Convection in a Parallel Plate Channel with a Centered Porous Layer, *Transport in Porous Media, 90* (2011), 3, pp. 791-806
[19] Ucar, E., *et al.*, Effect of an Inserted Porous Layer Located at a Wall of a Parallel Plate Channel on Forced Convection Heat Transfer, *Transport in Porous Media, 98* (2013), 1, pp. 35-57

Appendix

$$C_1 = (1-\xi)\frac{\mathrm{Gr_c}}{6\,\mathrm{Re}}(\theta_i - 1), \quad C_2 = \frac{\mathrm{Gr_c}}{6\,\mathrm{Re}} - \frac{\mathrm{Gr_c}\theta_i}{6\,\mathrm{Re}} + \frac{\mathrm{Gr_c}}{12\,\mathrm{Re}}(1+2\theta_i), \quad C_3 = \frac{\mathrm{Gr_c}(1+2\theta_i)}{12\,\mathrm{Re}(1-\xi)\,\mathrm{Re}},$$

$$C_4 = M\left(\frac{\mathrm{Gr_d}}{\mathrm{Re}} - 2\Gamma\right)$$

$$C_5 = 2\left(-M\frac{\mathrm{Gr_d}}{\mathrm{Re}}\theta_i + s^2 U_i + M\Gamma\right), \quad C_6 = -48 - (1-\xi)^3\left[\frac{\mathrm{Gr_c}}{\mathrm{Re}}(1-2\theta_i) + 2\frac{\mathrm{Gr_d}}{\mathrm{Re}}\right]$$

$$C_7 = 2(2-\xi)(-\xi)\frac{\mathrm{Gr_c}}{\mathrm{Re}}s^2(4\theta_i - 1) - 3\frac{\mathrm{Gr_d}}{\mathrm{Re}}\{4 - 8\theta_i + (-\xi)s^2[1 - 2\theta_i + 4(1-\xi)\theta_i]\}$$

$$C_8 = \left\{\begin{array}{l}\left[\xi s^4(-48 - (1-\xi)^3\left(\frac{\mathrm{Gr_c}}{\mathrm{Re}}(1-2\theta_i) + 4\frac{\mathrm{Gr_d}}{\mathrm{Re}}\theta_i\right)\right] \\ +4M\left[\begin{array}{l}2(1-\xi)\frac{\mathrm{Gr_c}}{\mathrm{Re}}s^2[-1 + (1-\xi) + 4\theta_i\xi] \\ +3\frac{\mathrm{Gr_d}}{\mathrm{Re}}[4 - 8\theta_i - \xi s^2(-1 + 2(1-\xi) + 2\theta_i)]\end{array}\right] +\end{array}\right\}$$

$$C_9 = 12((1-\xi)-1)M\left[\begin{array}{l}2(1-\xi)\dfrac{\mathrm{Gr_c}}{\mathrm{Re}}s^2(-1+(1-\xi)+4\theta_i-4(1-\xi)\theta_i)+\\ +3\dfrac{\mathrm{Gr_d}}{\mathrm{Re}}[8-16\theta_i+((1-\xi)-1)(1-\xi)s^2(1+2\theta_i)]\end{array}\right]+$$

$$+(1-\xi)s^2\left[-144s^2+(1-\xi)\left[144s^2+(1-\xi)\left(\begin{array}{l}12\dfrac{\mathrm{Gr_d}}{\mathrm{Re}}(-1+2\theta_i)+\\ +(1-\xi)-1)(1-\xi)(1-\xi)\dfrac{\mathrm{Gr_c}}{\mathrm{Re}}s^2(1+\theta_i)\end{array}\right)\right]\right]$$

$$C_{10} = 24[(1-\xi)-1]s^2,\ C_{11} = [-24M^2+12(1-\xi)Ms^2+(1-\xi)^4s^4]$$

$$C_{12} = 3M-3(1-\xi)(M+1)+(1-\xi)^3s^2$$

$$C_{13} = \left\{-12M\frac{\mathrm{Gr_d}}{\mathrm{Re}}[(1-\xi)-1-2\theta_i]+s^2\left[-48+(1-\xi)^3\frac{\mathrm{Gr_c}}{\mathrm{Re}}(2\theta_i-1)\right]\right\}$$

$$C_{14} = -12((1-\xi)-1)(1-\xi)\frac{\mathrm{Gr_d}}{\mathrm{Re}}s\left[(1-\xi)s+2\tanh\left(\frac{1}{2}(s-(1-\xi)s)\right)\right]+$$

$$+\sinh(s-(1-\xi)s)\left[\begin{array}{l}-12\left[\begin{array}{l}(1-\xi)^2+\\ +((1-\xi)-1)^2M\end{array}\right]\dfrac{\mathrm{Gr_d}}{\mathrm{Re}}s-3\left((1-\xi)-1)(16+(1-\xi)^3\dfrac{\mathrm{Gr_c}}{\mathrm{Re}}\right)s^3+\\ +2s\left(-12\left[\begin{array}{l}(1-\xi)^2(M-1)+M-\\ -2(1-\xi)M\end{array}\right]\dfrac{\mathrm{Gr_d}}{\mathrm{Re}}+5((1-\xi)-1)(1-\xi)^3\dfrac{\mathrm{Gr_c}}{\mathrm{Re}}s^2\right)\theta_i+\\ +4\left[\begin{array}{l}(1-\xi)^2\dfrac{\mathrm{Gr_c}}{\mathrm{Re}}s^2(-4\theta_i+1)-\\ -6(1-\xi)\dfrac{\mathrm{Gr_d}}{\mathrm{Re}}(1+M+2(M-1)\theta_i)\end{array}\right]\tanh\left(\frac{1}{2}(s-(1-\xi)s)\right)\end{array}\right]$$

$$C_{15} = \left\{\begin{array}{l}[-24M^2+12(1-\xi)Ms^2+(1-\xi)^4s^4]\cosh(s-(1-\xi)s)+\\ +4M\left[\begin{array}{l}6M-3(1-\xi)^2s^2+\\ +s(3M-3(1-\xi)(M+1)+(1-\xi)^3s^2)\sinh(s-(1-\xi)s)\end{array}\right]\end{array}\right\}$$

Paper submitted: October 1, 2012
Paper revised: April 24, 2013
Paper accepted: May 14, 2013